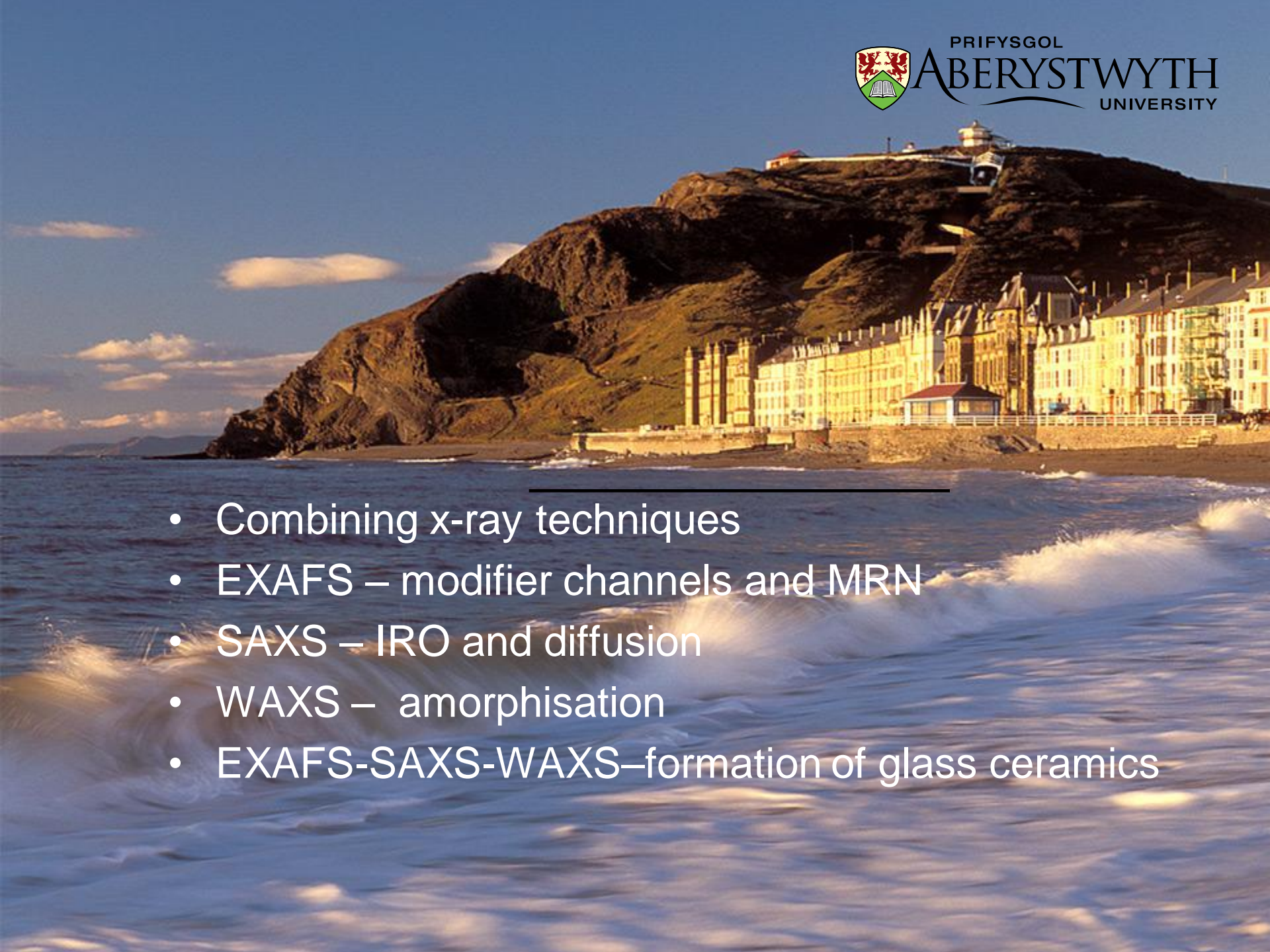


EXAFS-SAXS-WAXS

G.N. Greaves
*Institute of Mathematics and Physics,
Aberystwyth University,
Aberystwyth SY23 3BZ, UK*

GN Greaves and S Sen,
*Inorganic Glasses, Glass-Forming Liquids and Amorphising Solids,
Advances in Physics, 2007, 56, 1-166*

- 
- A scenic view of Aberystwyth University buildings along the coast, with a large cliff in the background and waves in the foreground. The buildings are illuminated by warm sunlight, and the sky is a clear blue with some light clouds.
- Combining x-ray techniques
 - EXAFS – modifier channels and MRN
 - SAXS – IRO and diffusion
 - WAXS – amorphisation
 - EXAFS-SAXS-WAXS–formation of glass ceramics

Combining x-ray techniques

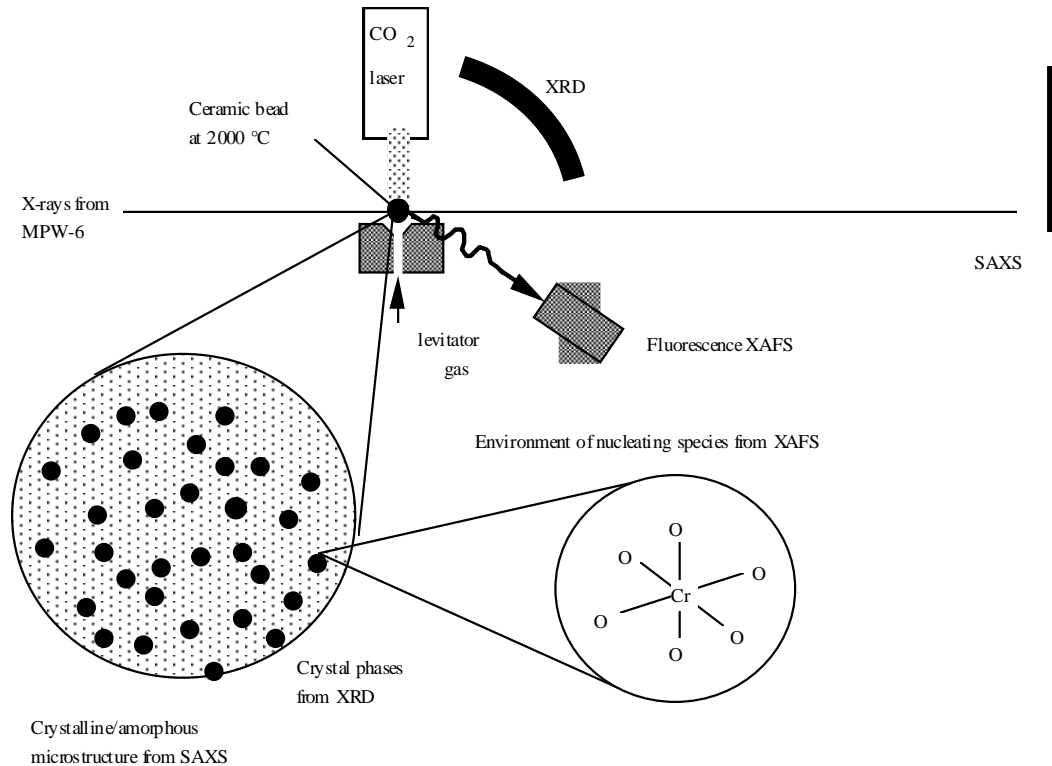
SAXS/WAXS

Bras W, Derbyshire G E, Ryan A J, Mant G R, Felton A, Lewis R A, Hall C J and Greaves G N
Nucl. Instr. and Methods. A326, 587-591 (1993)

EXAFS/WAXS

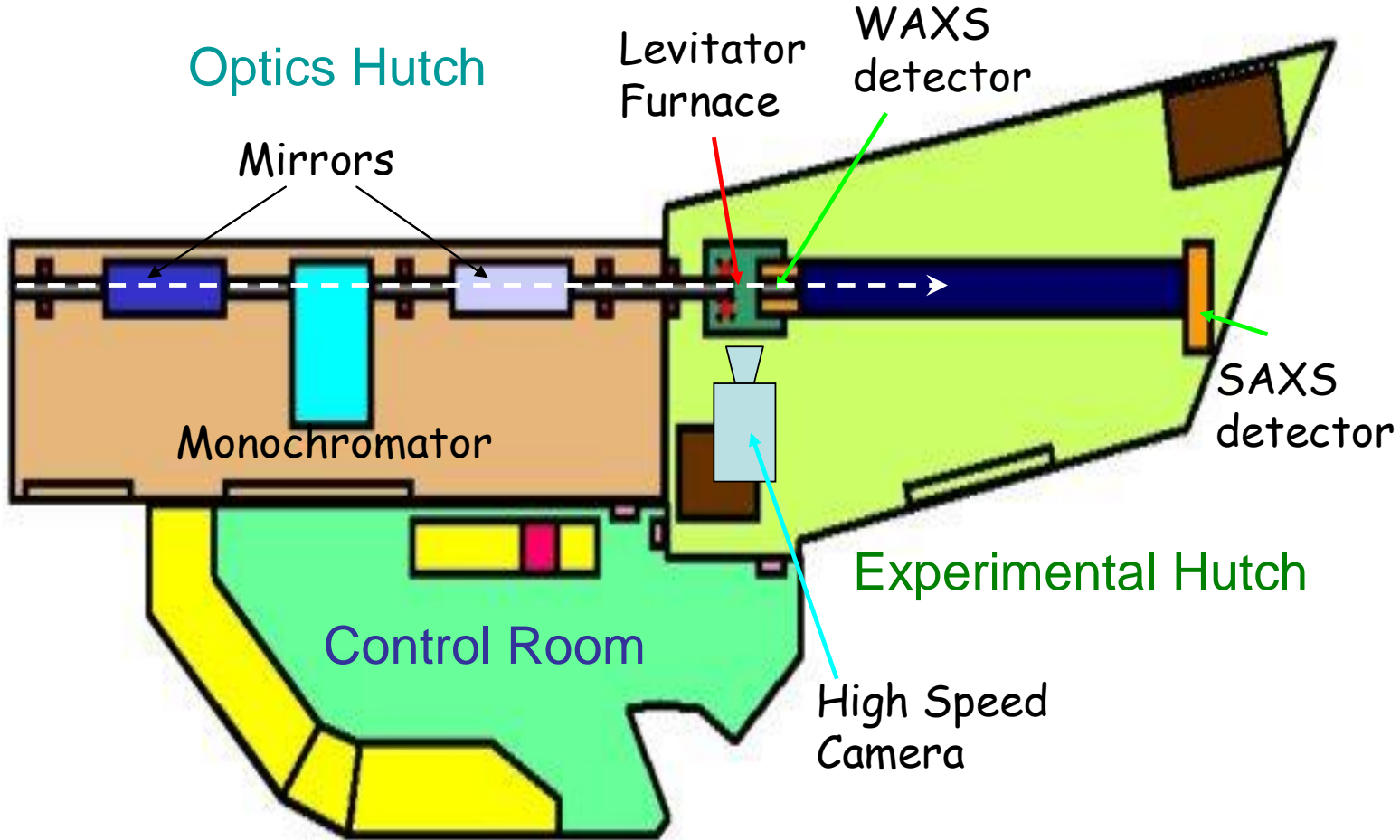
Sankar G, Wright P A, Srinivasa N, Thomas J M, Greaves G N, Dent A J, Dobson B R,
Ramsdale C A and Jones R H,
J. Phys. Chem. 97, 9550-9554 (1993)

combined x-ray techniques



Beamline 6.2 at Synchrotron Radiation Source

now moving to I22 at Diaampond Light Source



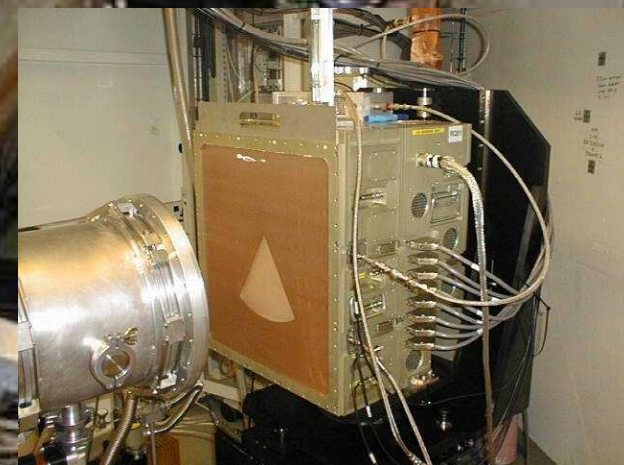
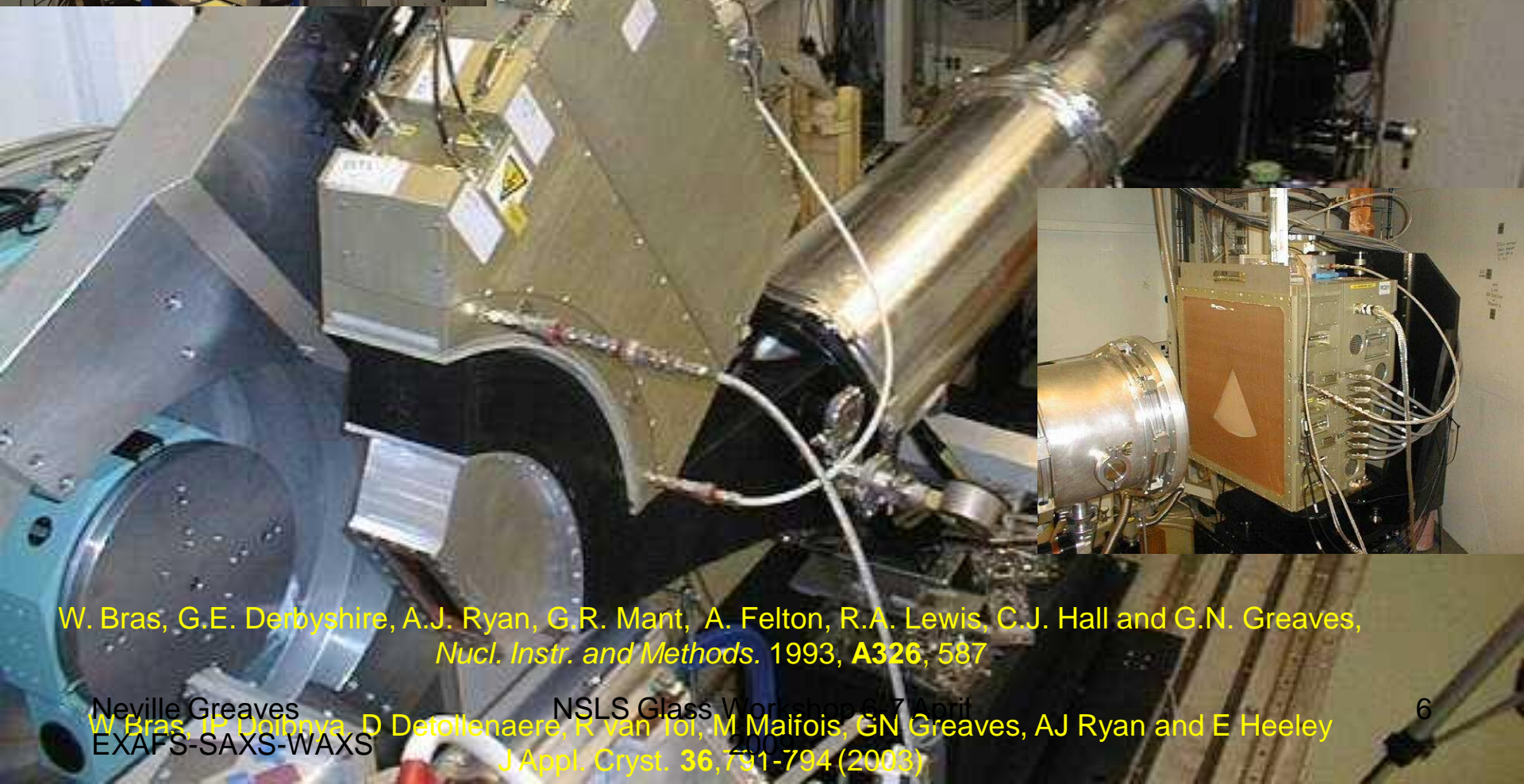
SAXS/WAXS



Prifysgol Cymru
Aberystwyth
The University of Wales

Combined small angle scattering and XRD

SRS 6.2, ESRF DUBBLE, I22 Diamond Light Source



W. Bras, G.E. Derbyshire, A.J. Ryan, G.R. Mant, A. Felton, R.A. Lewis, C.J. Hall and G.N. Greaves,
Nucl. Instr. and Methods. 1993, **A326**, 587

Neville Greaves
W. Bras, I.P. Dolbnya, D. Detollenaere
EXAFS-SAXS-WAXS

NSLS Glass Workshop 6-7 April

K van Tol, M Malfois, GN Greaves, AJ Ryan and E Heeley
J Appl. Cryst. 36, 791-794 (2003)

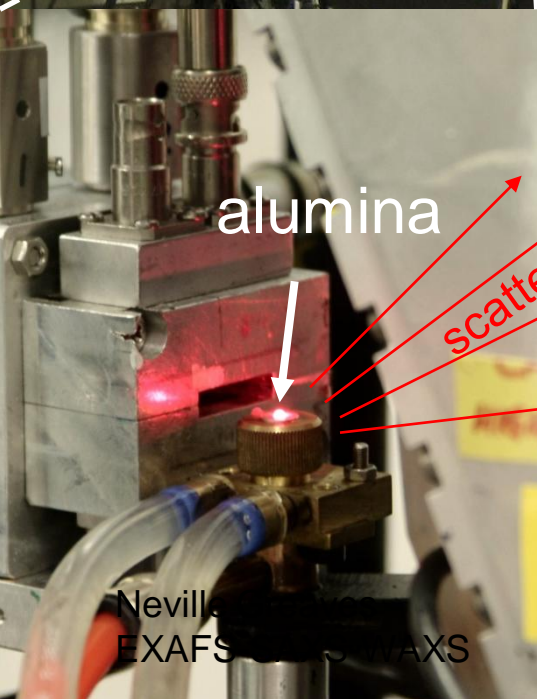


aerodynamic
levitator furnace
MPW6.2
furnace

Rapid2 WAXS

CO₂ laser

SAXS Camera



alumina

scattered x-rays

XRD of alumina in 0.1s
cooling at 10⁵ deg min⁻¹

EXAFS

Modifier channels and MRN

The Local Structure of Silicate Glasses

Greaves G N, Fontaine A, Lagarde P, Raoux D and Gurman S J
Nature, 293, p611-616 (1981)

Cation Microsegregation and Ionic Mobility in Mixed Alkali Glasses

Vessal B, Greaves G N, Marten P T, Chadwick A V, Mole R, Houde-Walter S
Nature 356, 504-507 (1992)

EXAFS - basics

Element specific:

Coordination Number, N

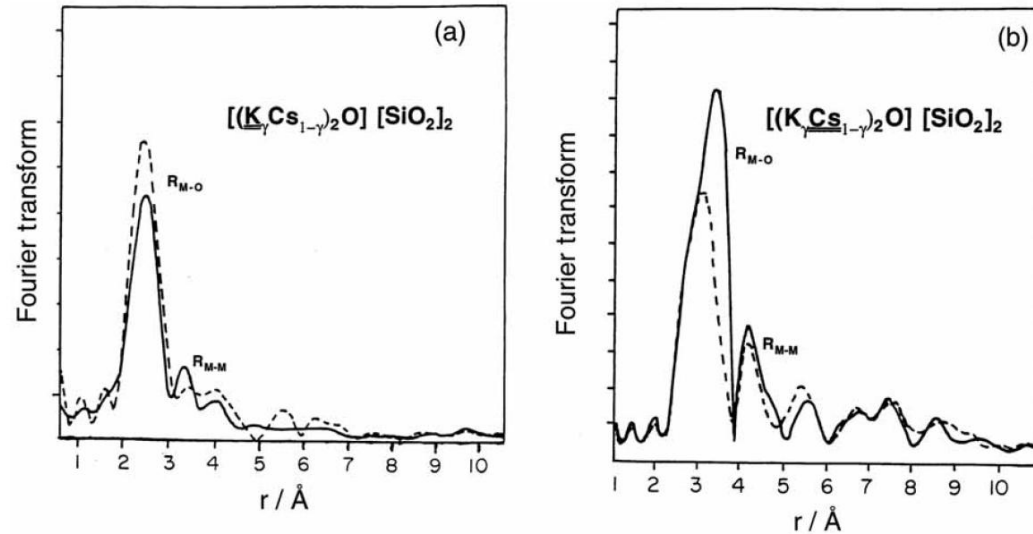
Inter-atomic Distance, R

Debye-Waller Factor, σ

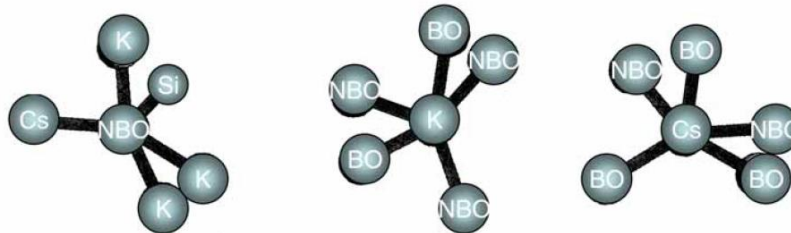
$$\chi(Q) = \sum_{\beta} \frac{A(Q)}{Q} \frac{N}{R_{\beta}^2} \left| f_{\beta}(Q, \pi) \right| \exp\left(-\frac{2R_{\beta}}{\lambda}\right) \exp\left(-2\sigma^2 Q^2\right) \sin\left(2QR_{\beta} + 2\delta + \phi\right)$$

N and R

Modifiers adopt well-defined sites in oxide glass networks



modifier polyhedra →

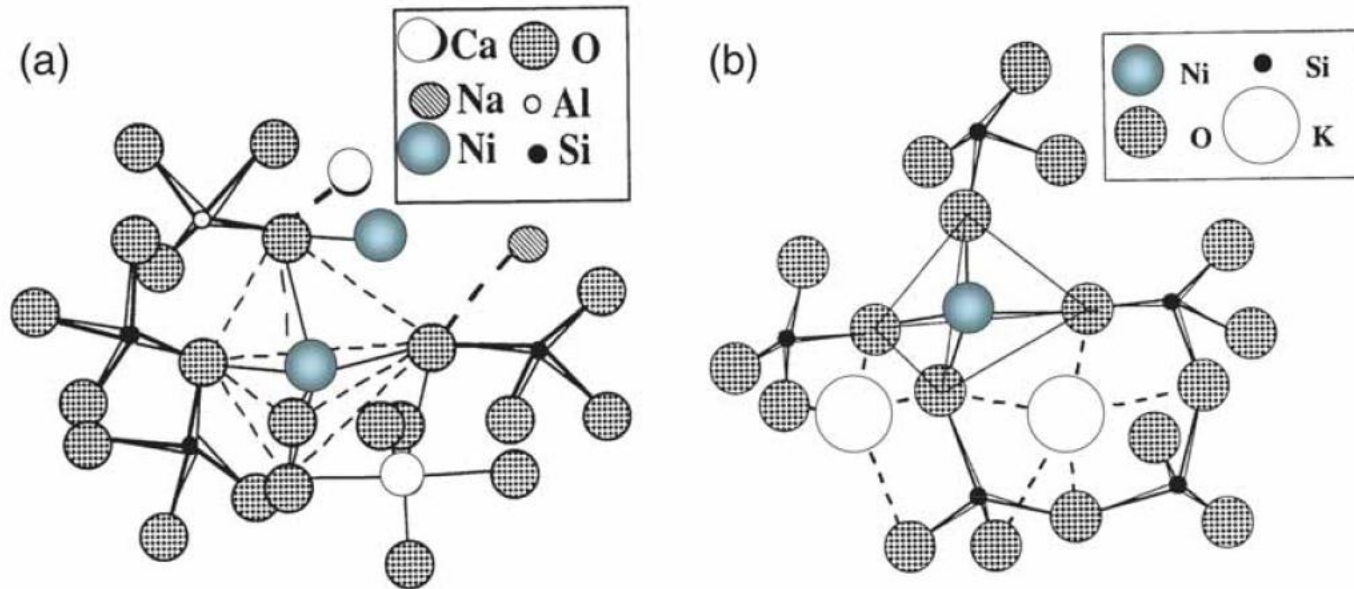


A Structural Basis for Ionic Diffusion in Oxide Glasses

Greaves G N, Gurman S J, Catlow C R A, Chadwick A V, Houde-Walter S,
Dobson B R and Henderson C M B
Phil. Mag. A65, 1059-1072 (1991)

N and R

Environments of intermediates in silicates



L. Galois and G. Calas, *Geochimica et Cosmochimica* **57** 3613 (1993); *ibid* **57** 3627.

(a)

modified random network

Molecular Dynamics

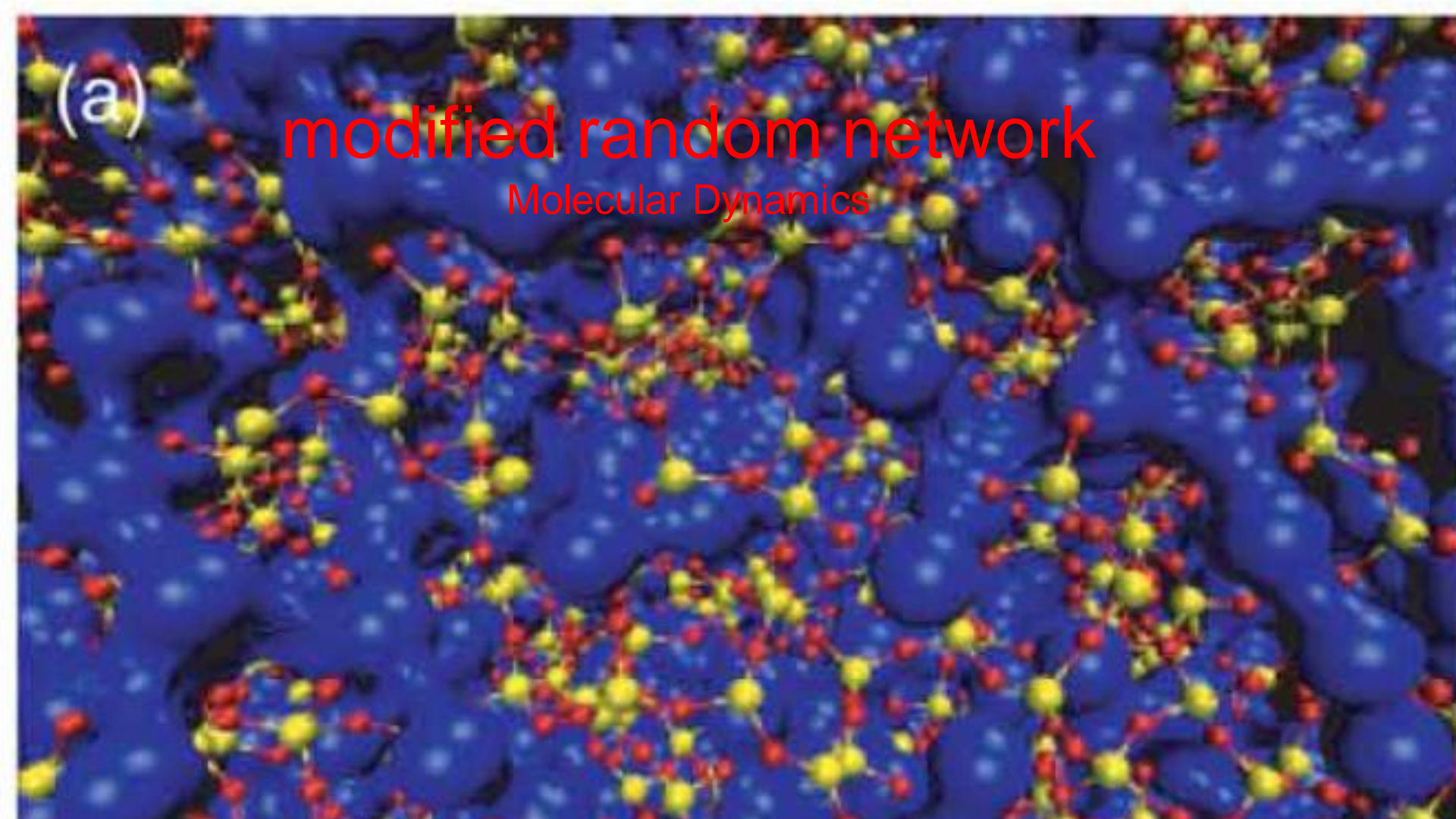


Figure 19. Static alkali channels modelled with molecular dynamics in alkali silicate glasses. (a) ‘Snapshot’ of the structure of the $\text{Na}_2\text{Si}_3\text{O}_7$ glass silicate with the Na atoms (blue) emphasized with an enlarged equipotential isosurface. Reproduced with permission from Meyer *et al.*

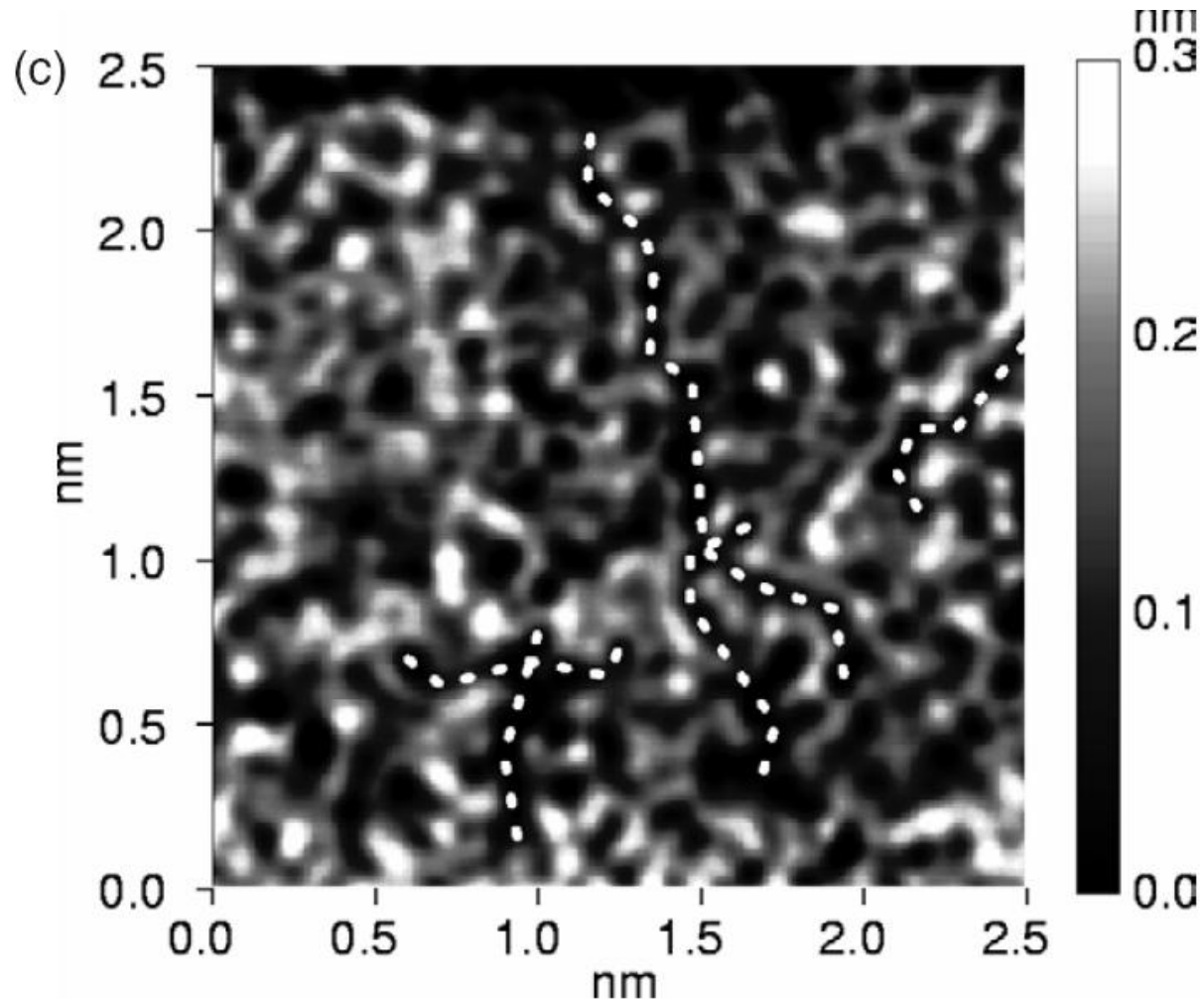
Meyer, J. Horbach, W. Kob, F. Kargl and H. Schobler, *Phys. Rev. Lett.* **93** 027801,1–4

(2004) Neville Greaves

NSLS Glass Workshop 6-7 April

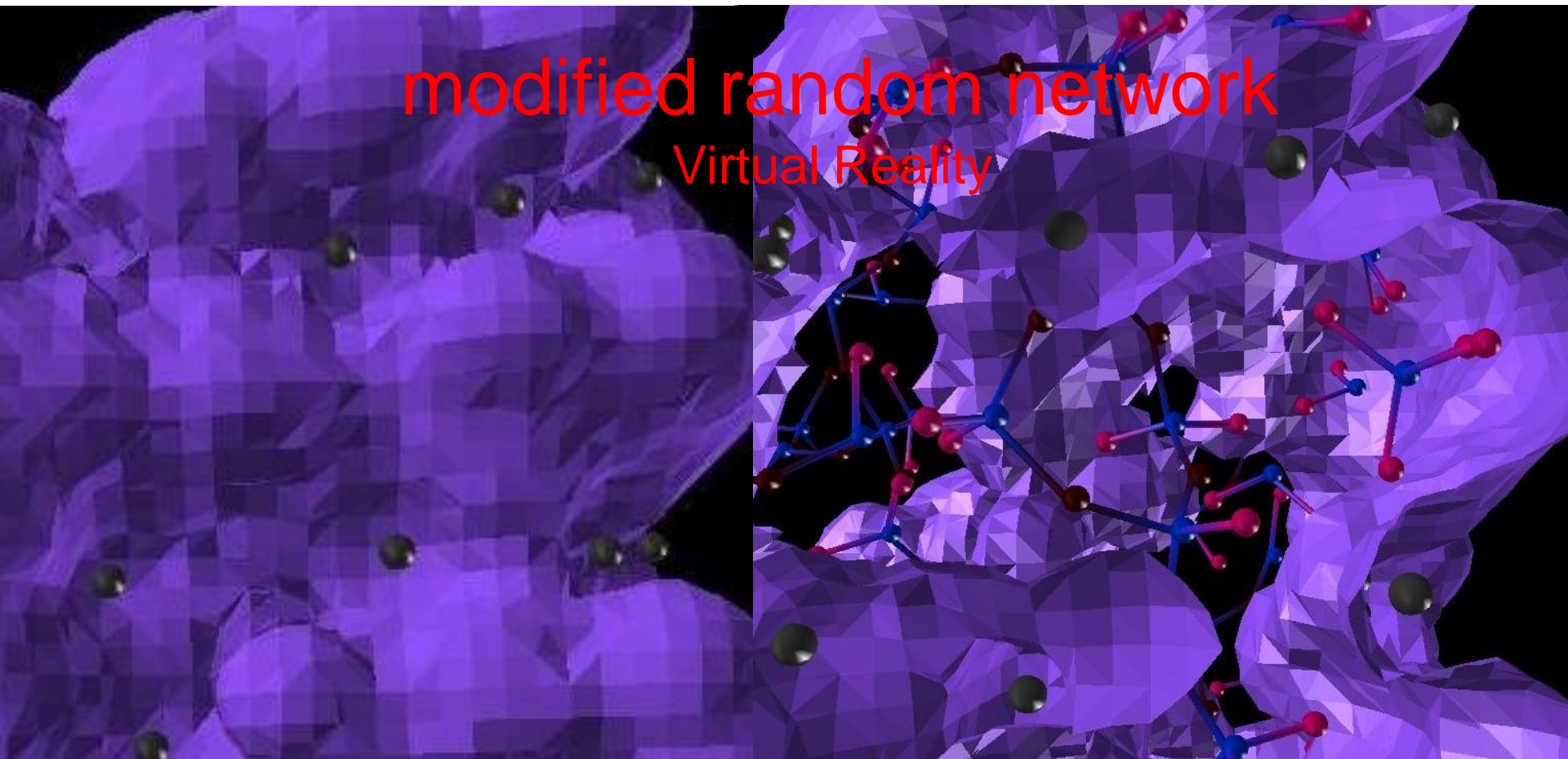
12

AFM modified random network



modified random network

Virtual Reality



network isosurface and cutaway for $\text{Na}_2\text{Si}_2\text{O}_5$

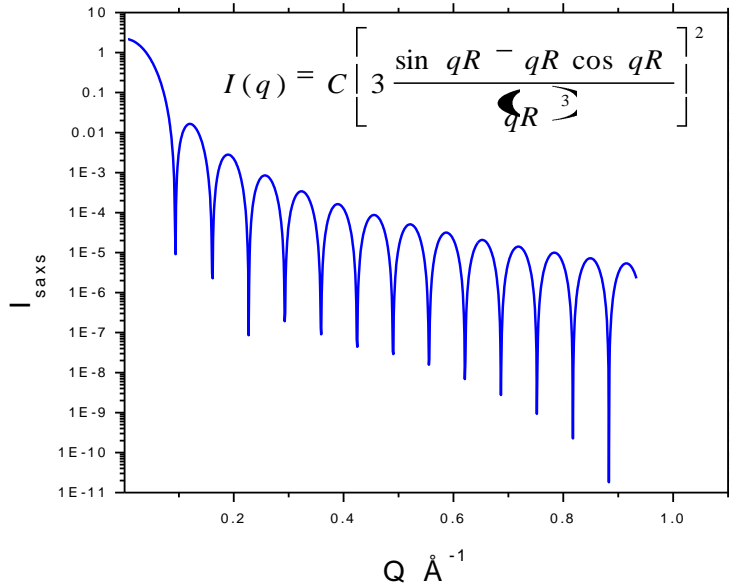
SAXS

Intermediate range order and diffusion Long Range order and LL Transitions

Inorganic Glasses, Glass-Forming Liquids and Amorphising Solids,
GN Greaves and S Sen,
Advances in Physics, 2007, 56, 1-166

G.N. Greaves, M.C. Wilding, S. Fearn, D. Langstaff, F. Kargl, S. Cox, Q. Vu Van, O. Majérus,
C.J. Benmore, R. Weber, C.M. Martin, L. Henet **Science** 2008, 322, 566-570.

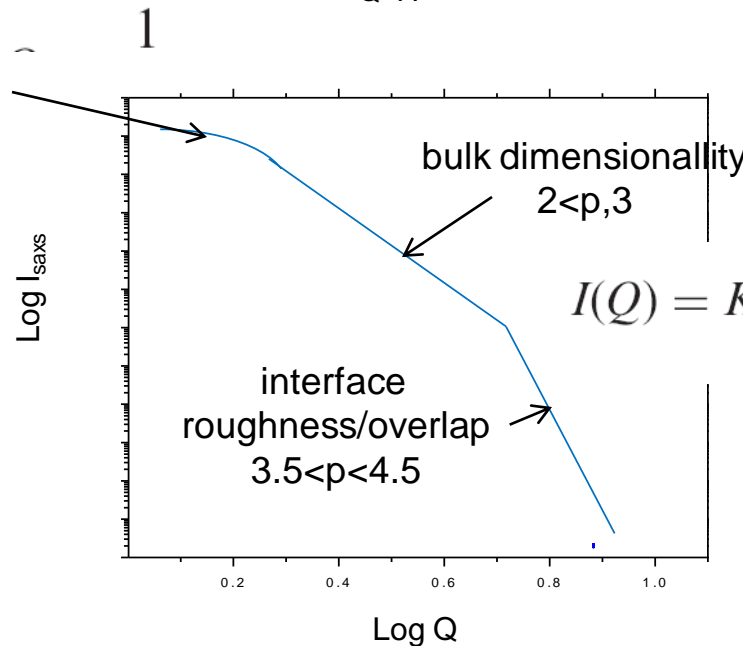
SAXS - basics



Guinier

$$I(Q) = I(0) e^{-R_{Rg}^2 Q^2 / 3}$$

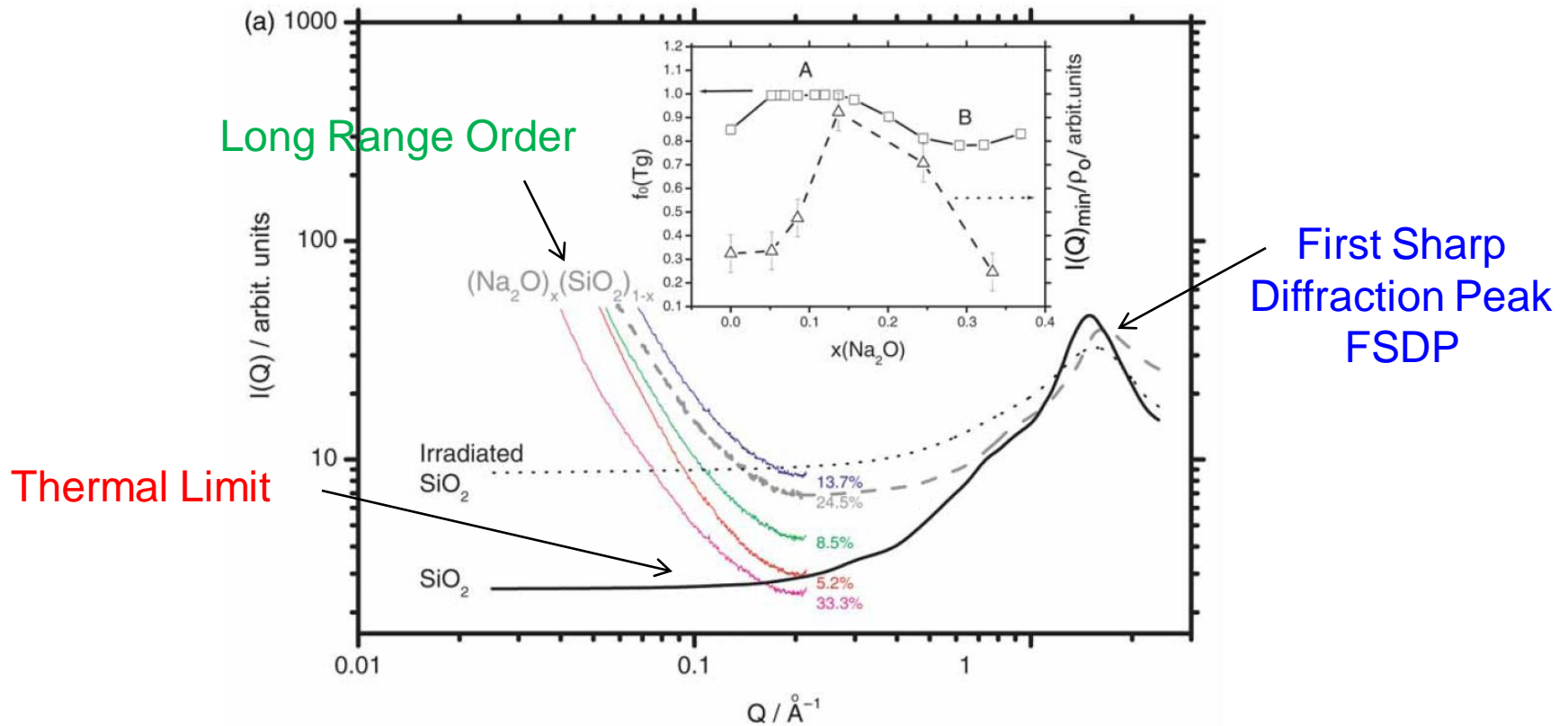
fractal structures



Porod

$$I(Q) = K_1 + \frac{K_2}{Q^p} \quad Q > \frac{1}{R_g}$$

SAXS and the Structure Factor, S(Q)



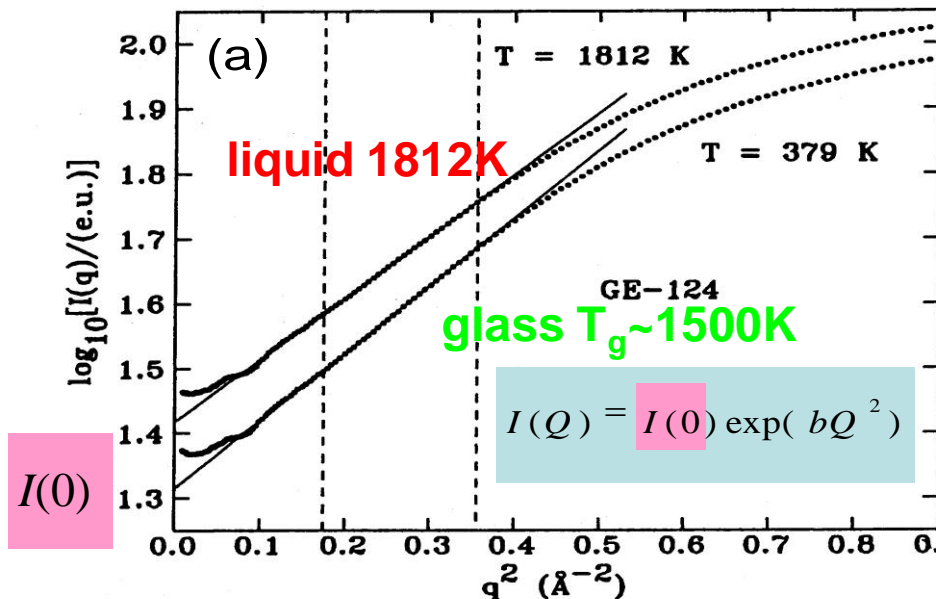
$$V \langle \Delta \rho^2 \rangle / \rho_0^2 = S(0) / \rho_0 = I(0) / (\rho_0 \sum_{\alpha}^N W_{\alpha\beta}^2 \dots) = k_B T K_T$$

density fluctuations & compressibility

SAXS from **liquid** and **glassy** SiO₂ **Q independent**

$$V \langle \Delta \rho^2 \rangle / \rho_0^2 = S(0) / \rho_0 = I(0) / (\rho_0 \sum_{\alpha} W_{\alpha}^2) = k_B T K_T$$

K_T, compressibility



R. Bruning, C. Levelut, A. Faivre, R. LeParc, J.-P. Simon, F. Bley, and J.-L. Hazemann: Europhys. Lett. Vol. 70, (2005), p.211.

V.V. Golubkov, J. Non-Cryst. Solids **192-193** 463 (1995).

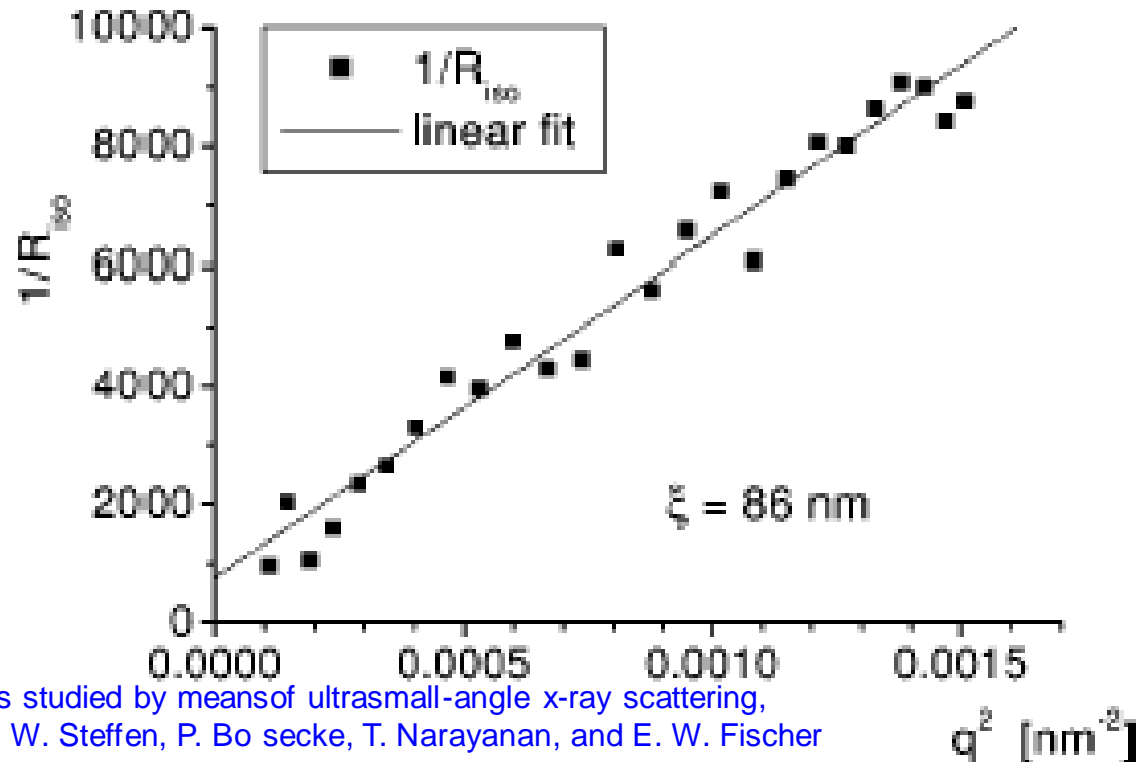
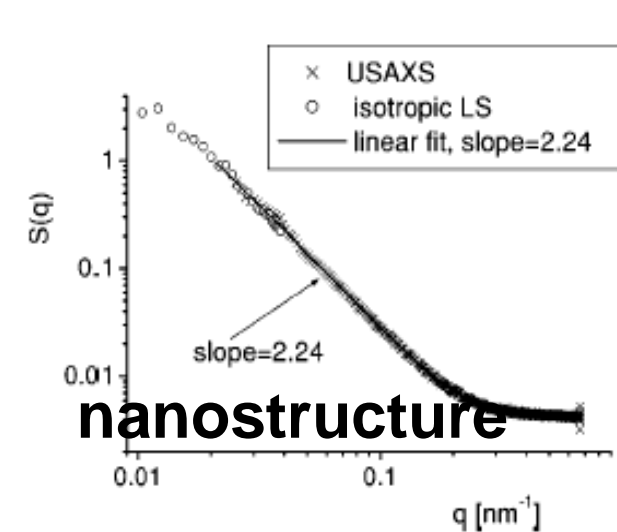
nanostructure & long range fluctuations in OTP

Ornstein-Zernike approximation

$$I(Q) = \frac{I_0}{1 + Q^2 \xi^2}$$

ξ correlation length

H.E. Stanley, Introduction to phase transitions and critical phenomena,
Oxford University press Oxford, 1971



Long-range density fluctuations in orthoterphenyl as studied by means of ultrasmall-angle x-ray scattering,
A. Patkowski, Th. Thurn-Albrecht, E. Banachowicz, W. Steffen, P. Bo secke, T. Narayanan, and E. W. Fischer
(2000) Phys Rev E, 61, 6909-6912

Yttria-alumina liquids & L-L Transitions

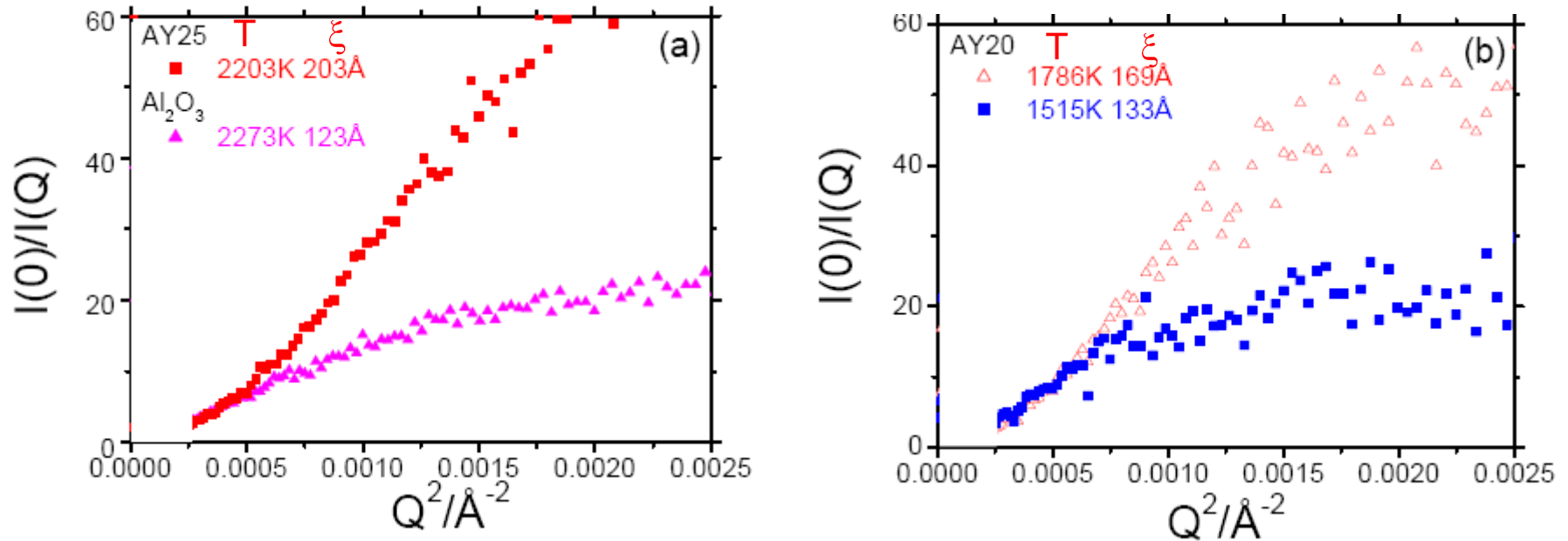


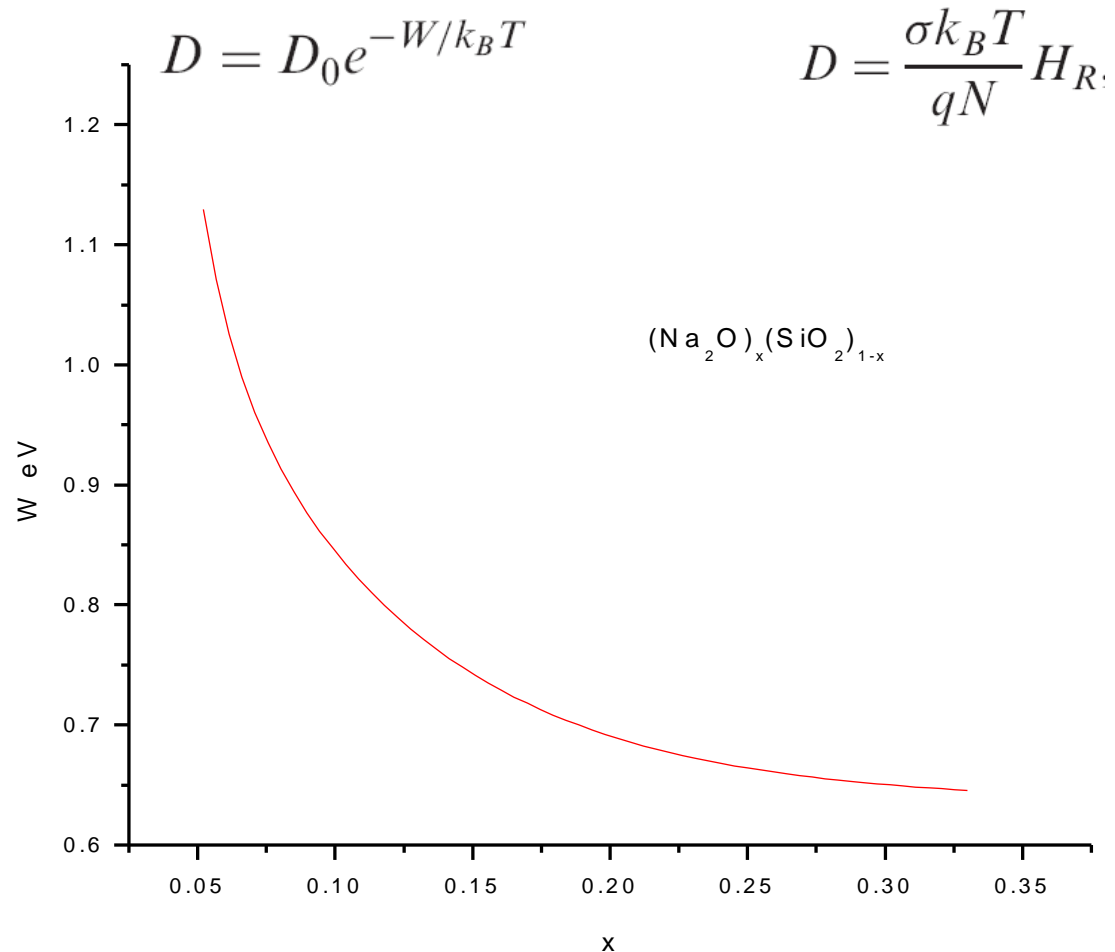
Fig. 6 Ornstein-Zernike plots of SAXS data $I(0)/I(Q) \propto Q^{-2}$, including the correlation lengths ξ of long range fluctuations analysed from the slopes at low Q for different temperatures. (a) SAXS data for liquid Al_2O_3 and AY25 at temperatures above T_m taken from Fig. 3(a) and the very different ξ values for these liquids of different strength. (b) AY20 data from Fig. 3(b), showing the increase in ξ at the liquid-liquid transition around 1788K (Fig. 4(a)) and the shift in the maximum to larger wavevectors.

$$I(Q) = \frac{I_0}{1 + Q^2 \xi^2} \quad \xi \text{ correlation length}$$

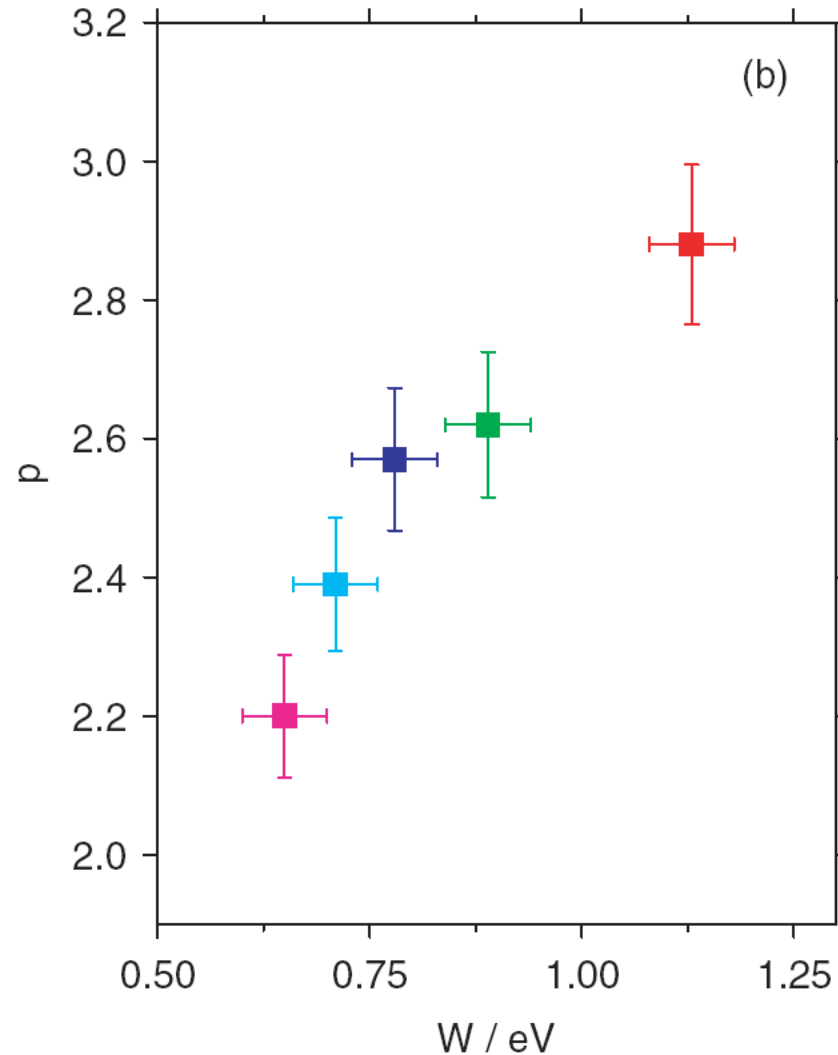
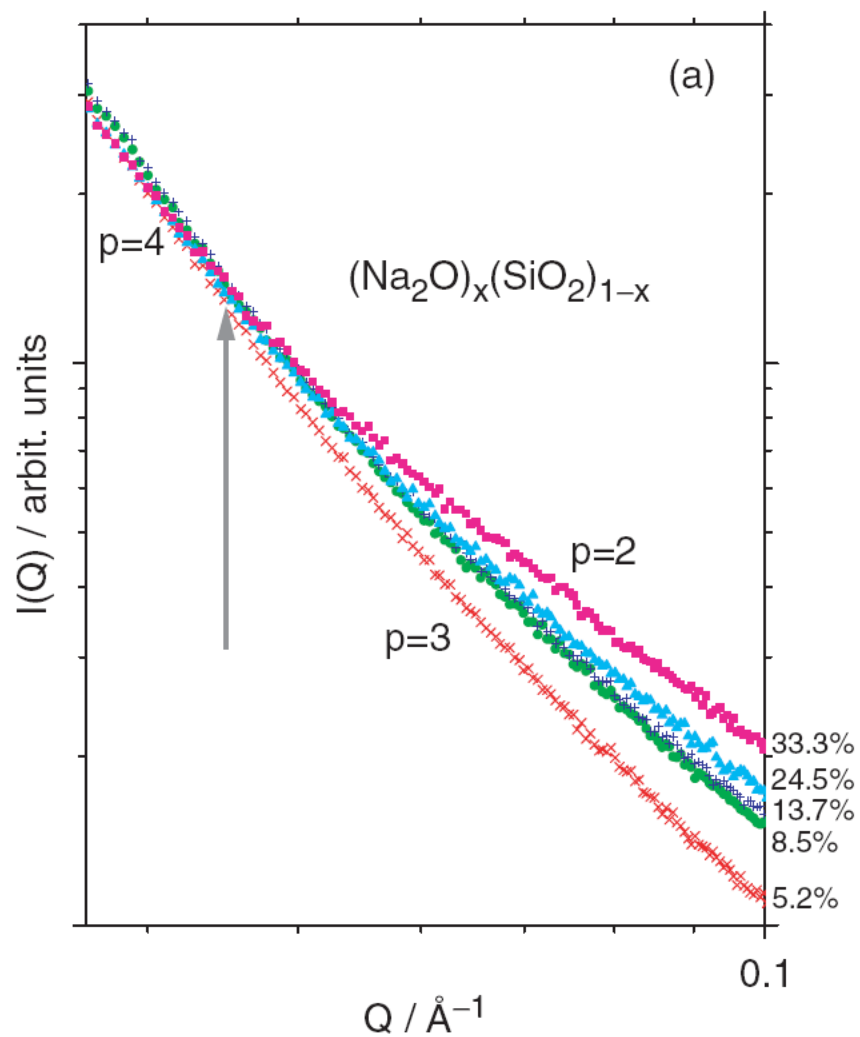
Liquid-liquid transitions, crystallisation and long range fluctuations in supercooled yttrium oxide-aluminium oxide. G.N. Greaves, M.C. Wilding, L. Hennet, W. Bras, O. Majérus, S. Fearn, F. Kargl
Journal of Non-Crystalline Solids (2009), doi:10.1016/j.jnoncrsol.2009.01.030

ionic diffusion/electrical conductivity

Single alkalis



SAXS and dimensionality and ionic diffusion



WAXS

partial structure factors

Inorganic Glasses, Glass-Forming Liquids and Amorphising Solids,
GN Greaves and S Sen,
Advances in Physics, 2007, 56, 1-166

WAXS - basics

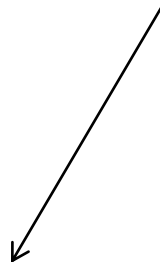
Element specific:

Structure Factor, $S(Q)$



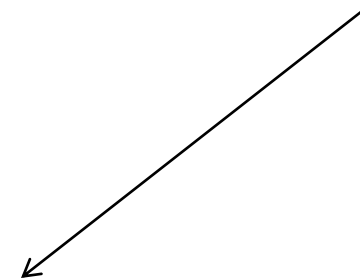
$$S(Q) = \sum_{\alpha} \sum_{\beta} W_{\alpha} W_{\beta} S_{\alpha\beta}(Q)$$

Partial Structure Factors, $S_{\alpha\beta}(Q)$



$$S_{\alpha\beta}(Q) = \frac{\sin(Qr_{\alpha\beta})}{Qr_{\alpha\beta}}$$

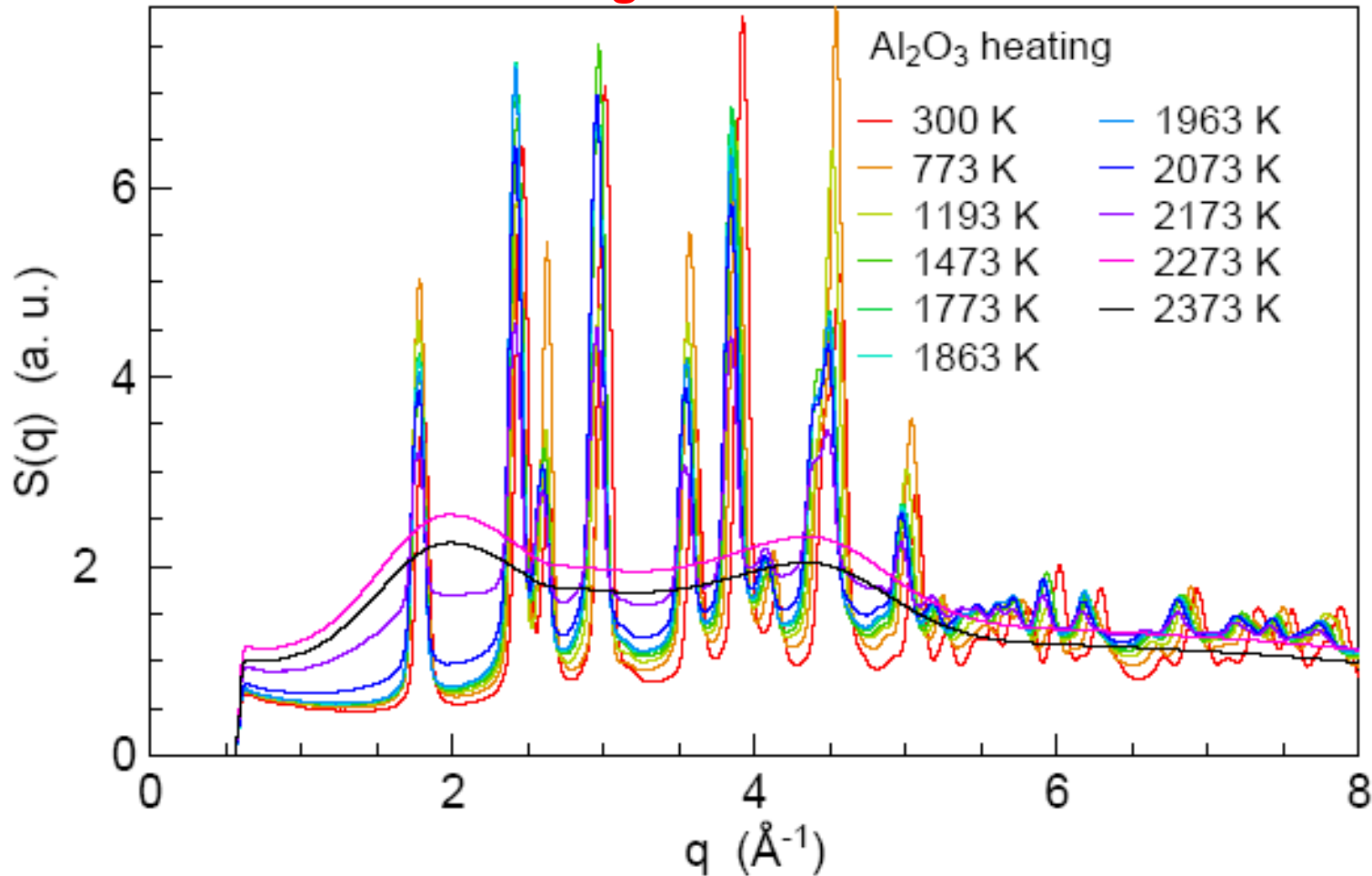
Radial Distribution Factor, $J(r)$



$$J(r) = \frac{2r}{\pi} \int_0^{\infty} [S(Q) - 1] \frac{\sin(Qr)}{Qr} dQ + 4\pi\rho_0 r^2$$

In situ X-ray Scattering and Diffraction

melting alumina ID16 ESRF



In situ structural studies of alumina during melting and freezing, G. N. Greaves, M. C. Wilding, S. Fearn, D. Langstaff, F. Kargl, Q. Vu Van, L.Hennet, I. Pozdnyakova, O. Majérus, *Advances in Synchrotron Radiation* (in press 2009)

Partial structure factors
in silica glass -
RMC from XRD and ND

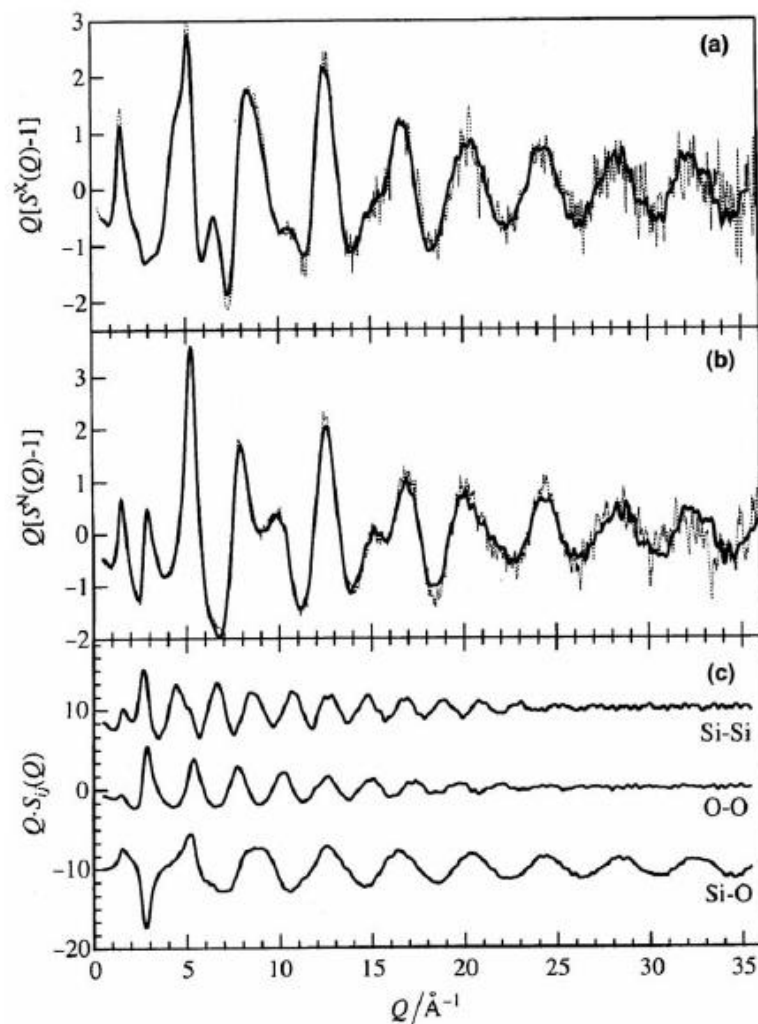


Figure 6. Reverse Monte Carlo simulation of silica glass compared to high-energy X-ray scattering (a) and neutron scattering (b). The interference functions, $Q(S(Q) - 1)$ differ because of the different cross-section weightings. Dashed lines are experimental and solid lines the result of RMC modelling. The partial structure factors for Si-Si, O-O and Si-O obtained from RMC modelling are given in (c), displaced vertically. Reproduced with permission from [60] © 2001 Elsevier.

H. Ohno, S. Kahara, N. Umesaki and K. Suzuya, *J. Non-Cryst. Solids* **293-295** 125 (2001).

Polyhedra in silicate glasses

EXAFS, ND and Molecular Dynamics

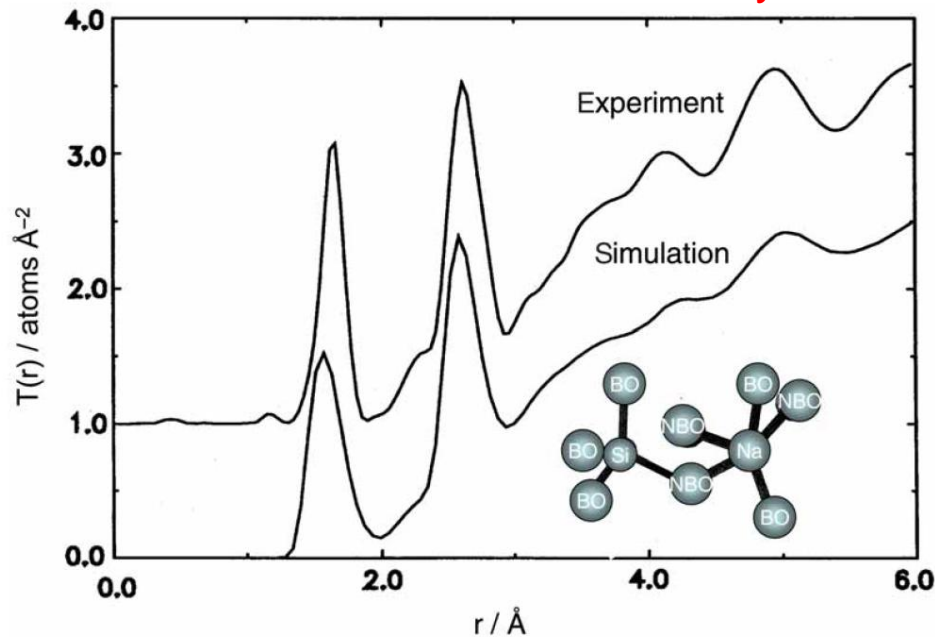


Figure 10. The total RDF $T(r) = J(r)/r$ (a) for $\text{Na}_2\text{Si}_2\text{O}_5$ glass obtained from neutron scattering (Exp) [132] compared to the predictions from an MD model (Sim) at 1000 K [125, 126]. A Si, Na, BO and NBO configuration is illustrated. Reproduced with permission from [126]

A Structural Basis for Ionic Diffusion in Oxide Glasses

Greaves G N, Gurman S J, Catlow C R A, Chadwick A V, Houde-Walter S, Dobson B Rand Henderson CMB
Phil. Mag. A65, 1059-1072 (1991)

Computer Simulation of Sodium Disilicate Glass

Smith W, Greaves GN and Gillan MJ
J. Chem. Phys. 103, 3091-3097 (1995)

Cation Microsegregation and Ionic Mobility in Mixed Alkali Glasses

Vessal B, Greaves G N, Marten P T, Chadwick A V, Mole R, Houde-Walter S
Nature 356, 504-507 (1992)

EXAFS-SAXS-WAXS

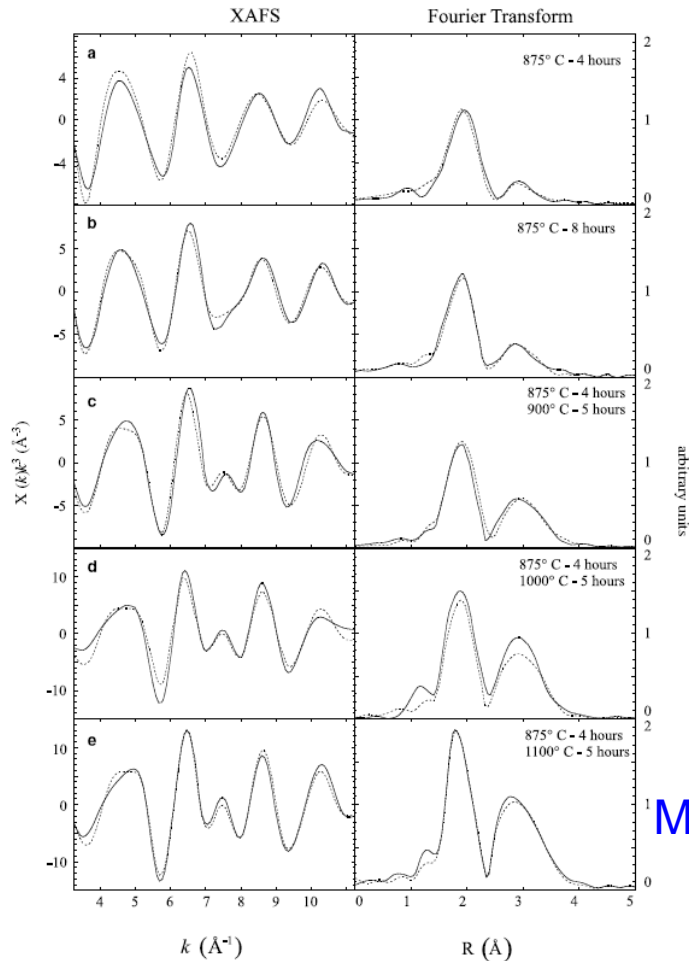
processing of glass ceramics

Bras, W.; Greaves, G. N.; Oversluizen, M.; Clark, S. M.; Eeckhaut, G. The development of monodispersed alumino-chromate spinel nanoparticles in doped cordierite glass, studied by in situ X-ray small and wide angle scattering, and chromium X-ray spectroscopy. *J. Non-Cryst. Solids* **2005**, *351* (27–29), 2178–2193.

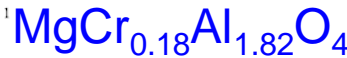
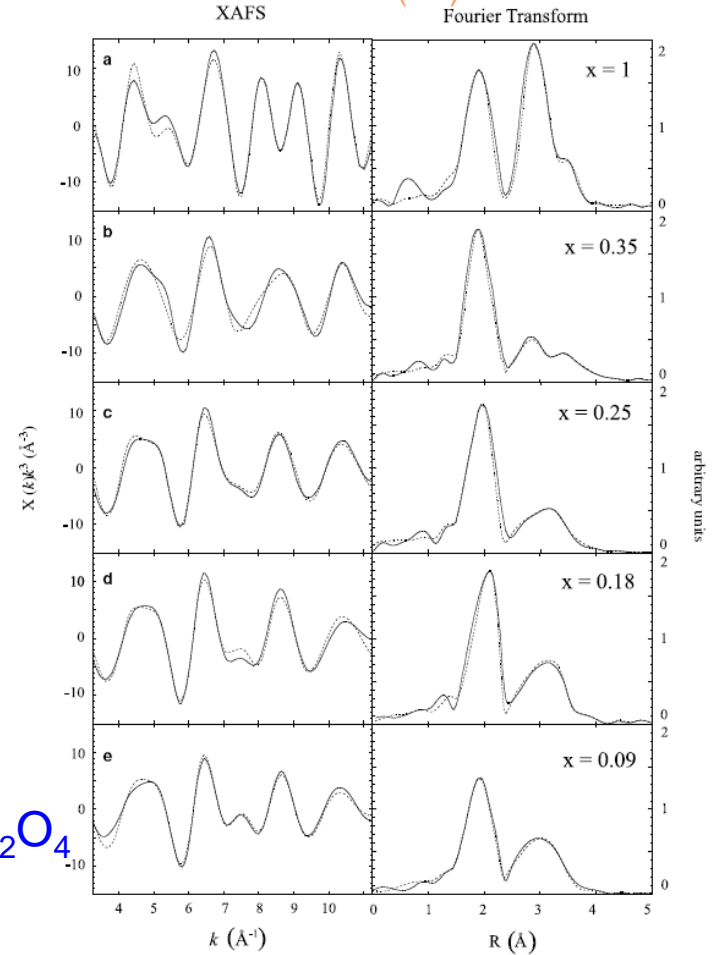
Bras, W, Clark, SM, Greaves, GN, Kunz, M, van Beek, W, Radmilovic, V, Nanocrystal growth in cordierite glass ceramics studied with x-ray scattering *Crystal Growth and Design*, doi: [10.1021/cg07056v](https://doi.org/10.1021/cg07056v) (in press 2009)

Cr EXAFS

cordierite ($\text{Mg}_2\text{Al}_4\text{Si}_5\text{O}_{18}$) glass
doped with 0.34 mol% Cr_2O_3

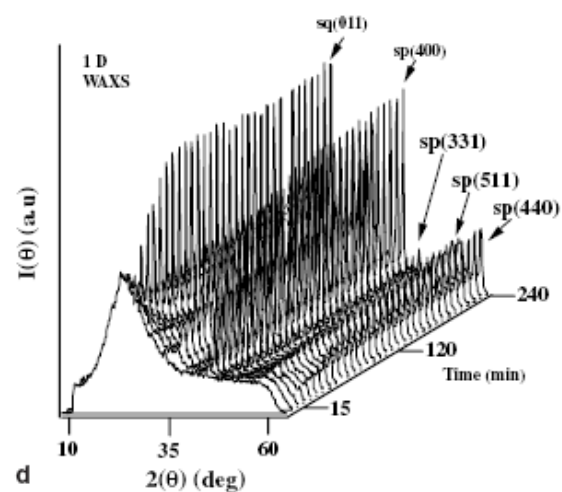
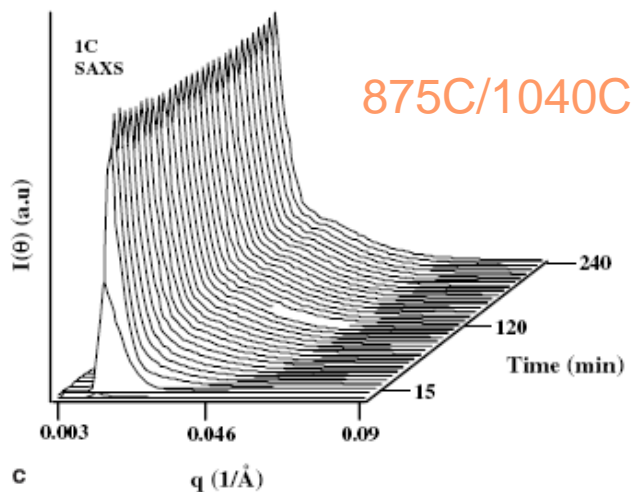
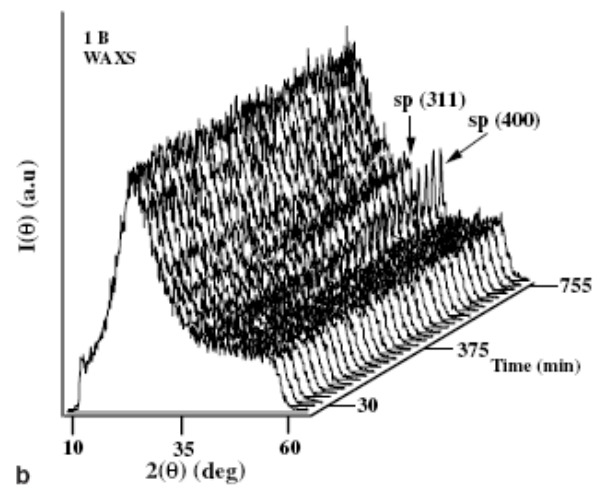
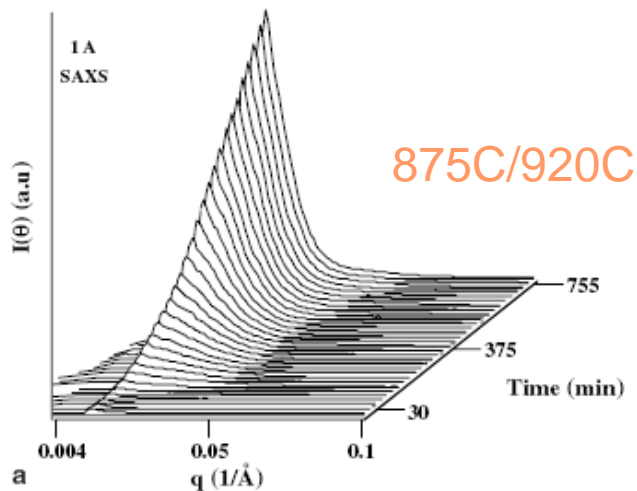


chromo-aluminate spinels
($\text{MgCr}_{2x}\text{Al}_{2(1-x)}\text{O}_4$)



cordierite ($\text{Mg}_2\text{Al}_4\text{Si}_5\text{O}_{18}$)
glass heat treated
at different temperatures

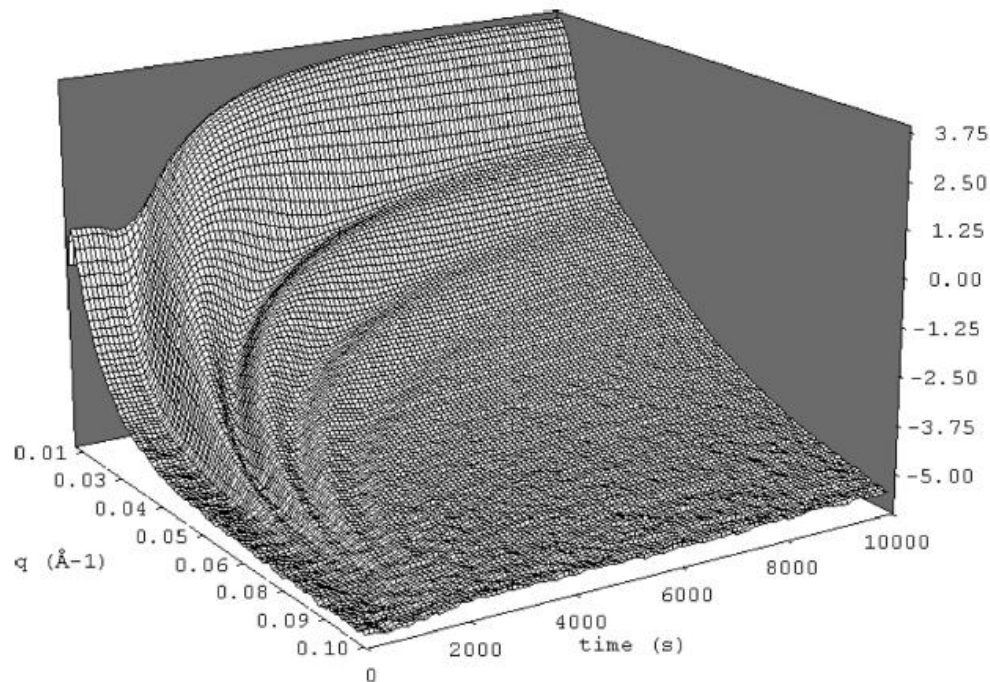
In situ SAXS/WAXS



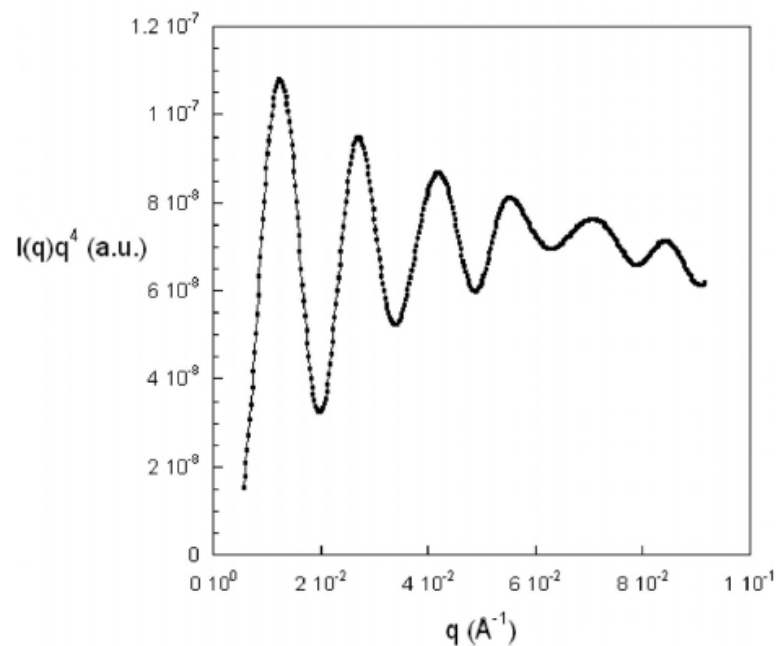
cordierite/Cr glass
875C/925C

SAXS and form factor

$\ln I_{\text{saxs}} \nu Q$



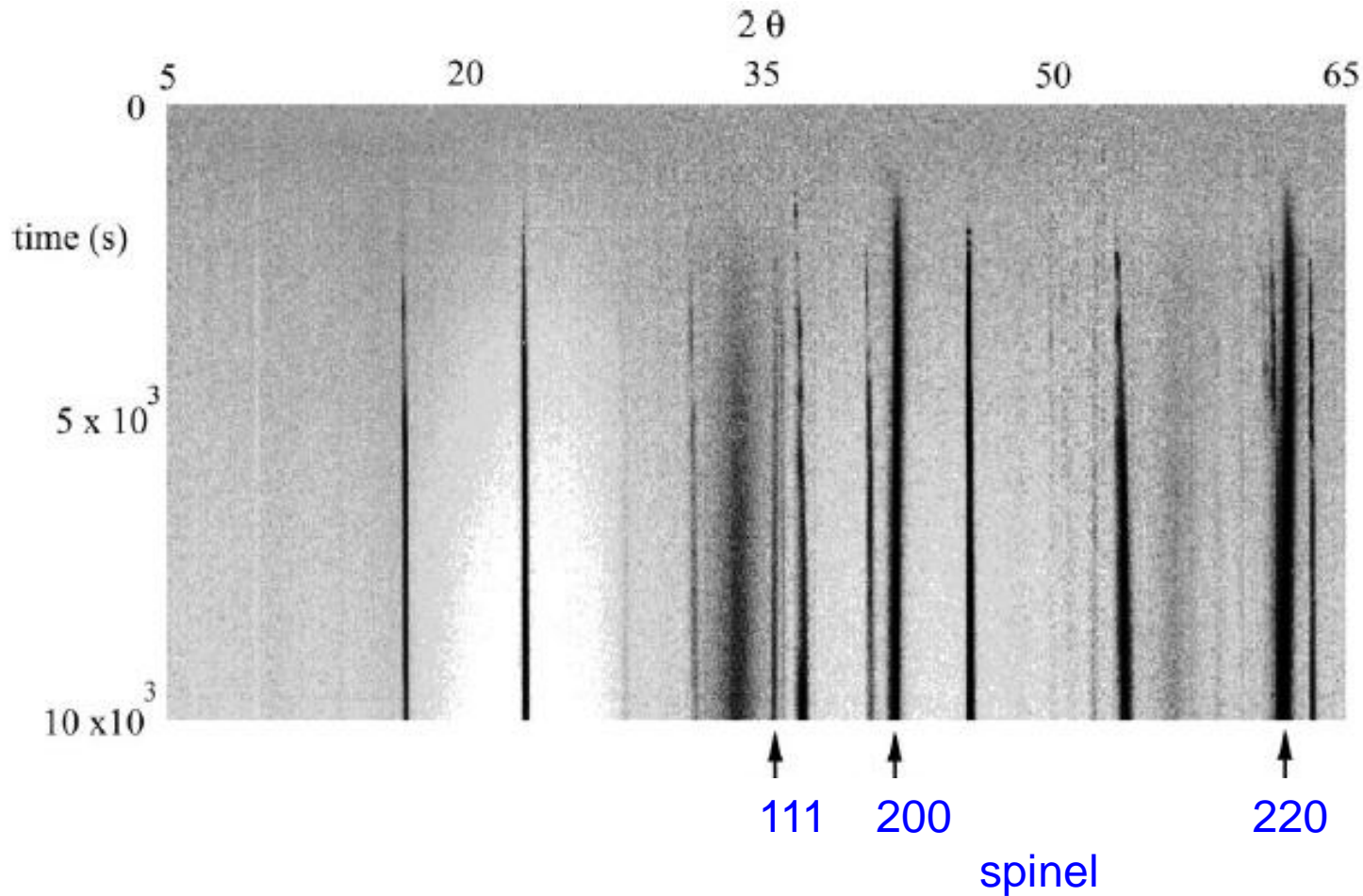
$I_{\text{saxs}} Q^4 \nu Q$
i.e with thermal fluctuations removed



20nm crystallites highly monodispersed

distinguishing nanocrystalline phases

spinel ($\text{MgCr}_{0.18}\text{Al}_{1.82}\text{O}_4$) in bulk & stuffed quartz (μ -cordierite) at surface



in situ spinel particle growth and internal strain

Guinier radius

$$R_g = \sqrt{\frac{3}{5}} R$$

Particle radius

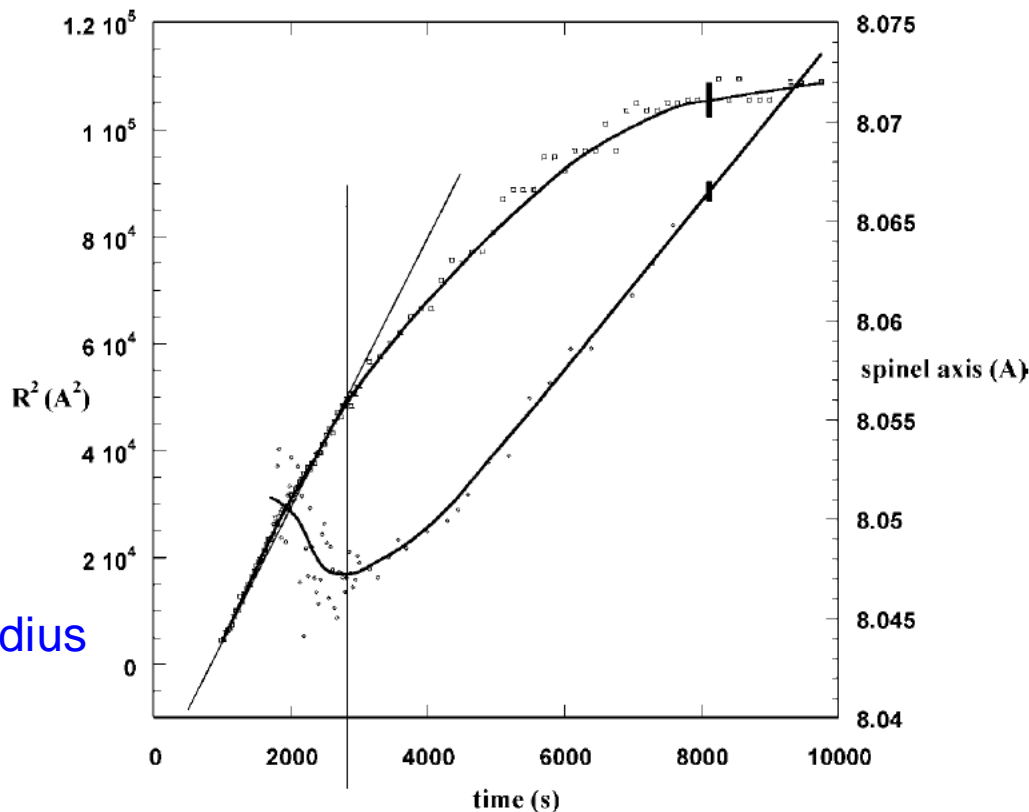



Figure 7. The correlation between the R^2 of the particle and time (\square). The vertical bar at time = 8000 s indicates the error margin at the later stages of development. At the early stages, a linear fit can be made to the R^2 data. This confirms the predictions that we are dealing with a diffusion-limited growth process. The development of the spinel unit cell volume as function of time (\diamond). The changeover from shrinking to growing coincides with the moment when the particle size leaves the $(t)^{1/2}$ growth regime. Also noteworthy is that this is the moment when the noise is much reduced.

- 
- Combining x-ray techniques
 - EXAFS – modifier channels and MRN
 - SAXS – IRO and diffusion
 - WAXS – amorphisation
 - EXAFS-SAXS-WAXS–formation of glass ceramics

